Separation Science and Technology
Publication details, including instructions for authors and subscription information:
http://www.informaworld.com/smpp/title~content=t713708471

Retention Time and the First Time Moment in Elution Chromatography. II. Analytical Solutions

Peter R. Rony[a]; James E. Funk[b]
[a] CORPORATE RESEARCH LABORATORIES ESSO RESEARCH AND ENGINEERING COMPANY, LINDEN, NEW JERSEY [b] COLLEGE OF ENGINEERING UNIVERSITY OF KENTUCKY LEXINGTON, KENTUCKY

To cite this Article Rony, Peter R. and Funk, James E.(1971) 'Retention Time and the First Time Moment in Elution Chromatography. II. Analytical Solutions', Separation Science and Technology, 6: 3, 383 — 399
To link to this Article: DOI: 10.1080/00372367108055563
URL: http://dx.doi.org/10.1080/00372367108055563

SEPARATION SCIENCE, 6(3), pp. 383–399, June, 1971

Retention Time and the First Time Moment in Elution Chromatography. II. Analytical Solutions

PETER R. RONY
CORPORATE RESEARCH LABORATORIES
ESSO RESEARCH AND ENGINEERING COMPANY
P. O. BOX 45
LINDEN, NEW JERSEY 07036

and

JAMES E. FUNK
COLLEGE OF ENGINEERING
UNIVERSITY OF KENTUCKY
LEXINGTON, KENTUCKY 40506

Summary

The relationships among the retention time, elution curve shape, and the zeroth and first partial normal moments are evaluated under conditions in which slight, moderate, or severe lateral mass transfer control exists. The elution curve and its moments are characterized by a single dimensionless group, ϕ, which is a measure of the rate of diffusional mass transfer into the stationary phase relative to the rate of mobile-phase convective mass transfer in the axial direction. Closed form solutions are given for a discrete description (a one-term approximation to the distributed description) of the stationary liquid phase. The dimensionless retention time is derived as a function of ϕ and the results compared to recently published experimental observations. The first normal moment is not invariant with respect to lateral kinetic phenomena when proper account is taken of the experimental restriction of a finite cutoff time.

INTRODUCTION

In a previous paper (*1*), we have derived and discussed the properties of the *column characteristic,* $\hat{G}$, an important transform quantity that contains all of the dynamic information of interest in elution chromatography. Such information may be extracted from $\hat{G}$ by taking successively higher normal moments. For example, the first normal moment, μ_1', for an impulse input can be calculated from (*1*),

$$\mu_1' = \frac{z}{v_1} + \frac{\epsilon_2}{\epsilon_1}\frac{z}{v_1} \lim_{p\to 0}\left(\hat{G} + p\,\frac{\partial \hat{G}}{\partial p}\right) \tag{1}$$

where z is set at L, the column length; v_1 is the velocity of the mobile phase; and ϵ_2/ϵ_1 is the ratio of the volume fractions of the stationary and mobile phases.

Certain problems exist in the interpretation of the normal moments, however, particularly when severe mobile-phase mass transfer control or stationary-phase diffusion control exists (*2*). For these conditions it is no longer possible to experimentally "integrate" to infinite time, as required by the formula for the mth normal moment,

$$\mu_m' = \frac{\int_0^\infty t^m c_{i1}\,dt}{\int_0^\infty c_{i1}\,dt} \tag{2}$$

As a consequence, the elution time of the chromatographic peak is no longer dictated by the equilibrium distribution coefficient. Little and Pauplis (*3*), Oberholtzer and Rogers (*4*), Kelley and Billmeyer (*5*), and Habgood and MacDonald (*6*) have recently described situations in which this type of phenomenon may exist.

It is the purpose of this paper to present numerical and analytical solutions to the conservation-of-mass equations characterizing a simple chromatographic system. The derivation of the general equations, such as Eqs. (1) or (3), has been presented in detail elsewhere (*1*). A significant result of our calculations is the fact that the shape of the elution curve is completely described by a single dimensionless group, ϕ, which is a measure of the rate of diffusion mass transfer into the stationary phase relative to the convective mobile-phase mass transfer in the axial direction. Although presented for a simple capillary column, the theoretical results can be extended to other situations if ϕ is properly interpreted.

IMPULSE RESPONSE

We have previously shown (*1*) that the elution output from a chromatographic column *for a unit impulse input* is given by

$$c_{i1}\left(L, t - \frac{L}{v_1}\right) = \mathcal{L}^{-1}\left\{\exp\left[-\frac{L}{v_1}\frac{\epsilon_2}{\epsilon_1} p\hat{G}\right]\right\} \qquad \left(t > \frac{L}{v_1}\right) \tag{3}$$

where $\hat{G}$, the column characteristic, is

$$\hat{G} \equiv \frac{\hat{c}_{i2|Av} + \hat{c}_{i3|Av}}{\hat{c}_{i1}} \tag{4}$$

$\hat{c}_{i1}$ is the Laplace transform of the concentration of component i in the mobile phase, and $\hat{c}_{i2}$ and $\hat{c}_{i3}$ are the Laplace transforms of the free and complexed component in the stationary phase. The subscript, Av, represents a lateral spatial average of the indicated quantities. The exponential parameter, γ, employed by Schneider and Smith (*7*) is closely related to $\hat{G}$.

For the simple capillary column shown in Fig. 1, the column characteristic is (*1*)

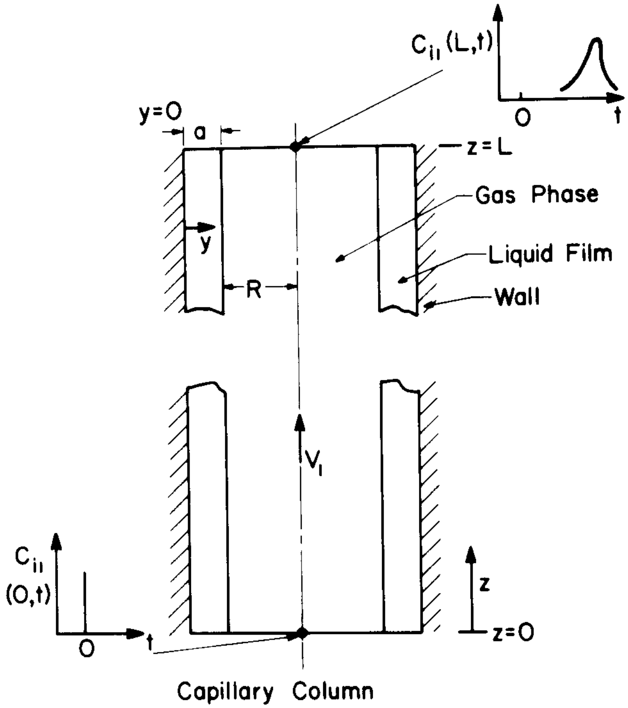

FIG. 1. Capillary chromatographic system.

$$\hat{G} = \kappa_{i2} \frac{\tanh qa}{qa} \qquad \text{Distributed liquid film} \tag{5}$$

$$\hat{G} = \kappa_{i2} \frac{\frac{8}{3}\frac{D_{i2}}{a^2}}{p + \frac{8}{3}\frac{D_{i2}}{a^2}} \qquad \text{Discrete approximation} \tag{6}$$

where

$$q^2 = \frac{p}{D_{i2}} \tag{7}$$

$$\frac{\epsilon_2}{\epsilon_1} \approx \frac{2a}{R} \qquad \text{for } a \ll R \tag{8}$$

Evaluation of the inverse transform given by Eq. (3) will furnish the elution curve which, with the aid of the convolution integral for Laplace transforms, can be used to determine the response to any type of column input.

The equations can be nondimensionalized by introducing the following variables

$$\tau = \frac{t - \frac{L}{v_1}}{t_0} \tag{9}$$

$$t_0 = 2 \frac{L}{v_1} \frac{a}{R} \kappa_{i2} \tag{10}$$

$$\phi = \frac{16}{3} \frac{L}{v_1} \frac{a}{R} \kappa_{i2} \frac{D_{i2}}{a^2} \tag{11}$$

The characteristic time, t_0, is that contribution to the first normal moment made by the mass transfer process, and the parameter ϕ is a measure of the rate of diffusional mass transfer into the liquid film relative to the rate of mass transfer by convection in the axial direction.

With these changes of variables, the impulse response becomes

$$t_0 c_{i1}(L,\tau) = \mathcal{L}^{-1} \left\{ \exp \left(-p \frac{\tanh \sqrt{\frac{8p}{3\phi}}}{\sqrt{\frac{8p}{3\phi}}} \right) \right\} \tag{12}$$

for the distributed liquid film and

$$t_0 c_{i1}(L,\tau) = \mathcal{L}^{-1}\left\{\exp\left(-\frac{\phi p}{p+\phi}\right)\right\} \tag{13}$$

for the discrete liquid film. The dimensionless elution curves given by Eqs. (12) and (13) are completely determined by the parameter ϕ.

SOLUTION FOR DISTRIBUTED LIQUID FILM

We were unable to obtain a closed form solution of the inversion indicated in Eq. (12). A numerical inversion was obtained, however, and is shown in Figs. 2 and 3 for two different values of ϕ. The solid lines give the numerical results for the distributed liquid film model, whereas the dashed lines are analytical solutions for a discrete description of the liquid film that will be discussed in the following section.

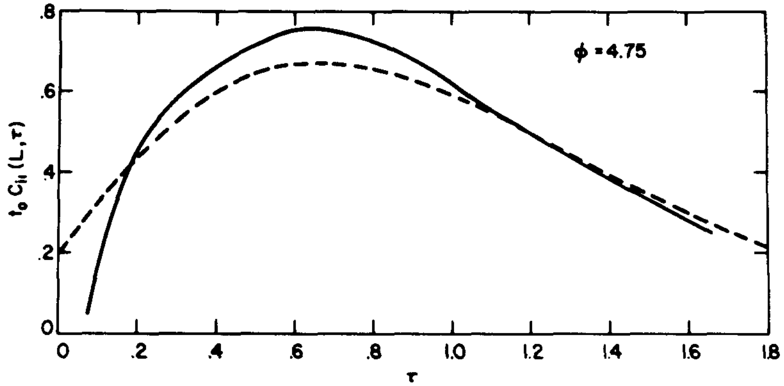

FIG. 2. Solutions to Eq. (12) [solid line] and Eq. (13) [dashed line] for $\phi = 4.75$.

Wing's method for the inversion of Laplace transforms (*8*) was employed. We encountered problems in the a priori selection of certain of the parameters required for the numerical inversion. For this and other reasons that will become evident later, the analytical solution was preferred even though it was only an approximation to the true solution.

SOLUTION FOR DISCRETE LIQUID FILM

We have previously shown that the discrete description of the liquid film—a variation of the lumping procedure originally described

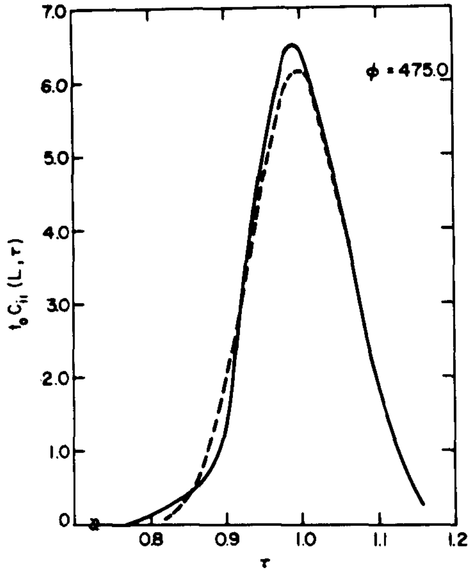

FIG. 3. Solutions to Eq. (12) [solid line] and Eq. (13) [dashed line] for $\phi = 475$.

by Funk and Houghton (*9*)—is, in a sense, a one-term approximation to the distributed model, and have suggested a procedure for the determination of ϕ via a single-stage experiment (*1*). By means of the substitution theorem for Laplace transforms, Eq. (13) becomes

$$t_0c_{i1}(L,\tau) = \begin{cases} 0 & \tau < 0 \\ e^{-\phi(1+\tau)}[t_0\delta(t_0\tau) + \mathcal{L}^{-1}\{e^{\phi^2/p} - 1\}] & \tau \geq 0 \end{cases} \tag{14}$$

The inverse transform of Eq. (14) is given in the Bateman tables (*10*),

$$\mathcal{L}^{-1}\{e^{\phi^2/p} - 1\} \equiv \frac{\phi}{\tau^{1/2}} I_1(2\phi\tau^{1/2}) \tag{15}$$

Therefore, the final desired solution is

$$t_0c_{i1}(L,\tau) = \begin{cases} 0 & \tau < 0 \\ e^{-\phi(1+\tau)}\left[t_0\delta(t_0\tau) + \dfrac{\phi}{\tau^{1/2}} I_1(2\phi\tau^{1/2})\right] & \tau \geq 0 \end{cases} \tag{16}$$

where $(t_0\tau)$ is a unit impulse at $\tau = 0$ and I_1 is the modified Bessel function of order unity.

Equation (16) is shown as the dashed line in Figs. 2 and 3. The information contained in the elution curves is more easily and accurately obtained from Eq. (16) than from the numerical inversion. The ease in handling and the flexibility of a closed form solution is clearly preferable to the numerical inversion results.

The first term in the brackets in Eq. (16) represents an impulse at $\tau = 0$, corresponding to the column transport time of L/v_1. The integrated area of this impulse is $e^{-\phi}$, which is the fraction of the component that has passed through the chromatographic column without permeating the stationary phase. This fraction has a value of unity when $\phi = 0$ and a value of zero when $\phi \rightarrow \infty$. The second part of the elution curve described by Eq. (16) is a skew Gaussian or a decaying exponential for all $\tau > 0$ and $\phi \neq 0$.

Elution curve profiles, corresponding to Eq. (16), for various values of ϕ are given elsewhere (*2*). For $\phi = 0$, the response to a unit impulse is likewise a unit impulse at $\tau = 0$. As the value of ϕ is increased, the magnitude of the impulse at $\tau = 0$ decreases and, for $\phi > 2$, a peak maximum develops. As ϕ is increased beyond 2, the peak maximum moves toward $\tau = 1$ and the elution curve sharpens. The elution curve approaches a unit impulse at $\tau = 1$ when ϕ becomes very large. The over-all type of behavior is shown *schematically* in Fig. 4.

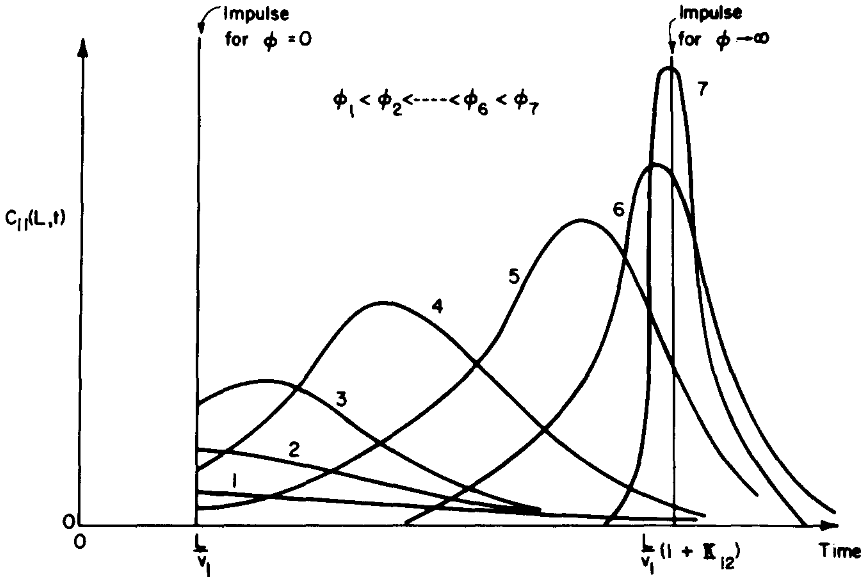

FIG. 4. Schematic behavior of elution curves as a function of ϕ. K_{12} is a gas–liquid distribution coefficient (*2*).

PARTIAL NORMAL MOMENTS

We have previously defined the *partial normal statistical moment*, $\tilde{\mu}_m$, as (*2*)

$$\tilde{\mu}_m \equiv \frac{\int_0^{t_c} t^m c_{i1}(L,t)\,dt}{\int_0^{\infty} c_{i1}(L,t)\,dt} \tag{17}$$

For the system described in this paper, $\tilde{\mu}_m$ becomes

$$\tilde{\mu}_m = \int_{\frac{L}{v_1}}^{t_c} t^m c_{i1}(L,t)\,dt = t_0^m \int_0^{\tau_c} \left(\tau + \frac{L/v_1}{t_0}\right)^m t_0 c_{i1}(L,\tau)\,d\tau \tag{18}$$

where τ_c is a dimensionless cutoff time,

$$\tau_c \equiv \frac{t_c - \dfrac{L}{v_1}}{t_0} \tag{19}$$

From Eq. (16), we first obtain

$$\tilde{\mu}_0 = e^{-\phi} + \int_0^{\tau_c} e^{-\phi(1+\tau)} \frac{\phi}{\tau^{1/2}} I_1(2\phi\tau^{1/2})\,d\tau \tag{20}$$

and

$$\tilde{\mu}_1 = \frac{L}{v_1}\tilde{\mu}_0 + t_0 \int_0^{\tau_c} e^{-\phi(1+\tau)}\phi\tau^{1/2} I_1(2\phi\tau^{1/2})\,d\tau \tag{21}$$

for the zeroth and first partial normal moment, respectively. With the aid of Eq. 813.3 in Dwight's tables (*11*),

$$I_1(2\phi\tau^{1/2}) \equiv \phi\tau^{1/2} \sum_{n=0}^{\infty} \frac{\phi^{2n}\tau^n}{n!(n+1)!} \tag{22}$$

and the following gamma function definitions,

$$\gamma(n+1,\nu_c) = \int_0^{\nu_c} v^n e^{-v}\,dv \tag{23}$$

$$\gamma(n+2,\nu_c) = \int_0^{\nu_c} v^{n+1} e^{-v}\,dv \tag{24}$$

where

$$v = \phi\tau \tag{25}$$

$$\nu_c = \phi\tau_c \tag{26}$$

Eqs. (19) and (20) become

$$\tilde{\mu}_0 = e^{-\phi} + \phi e^{-\phi} \sum_{n=0}^{\infty} \frac{\phi^n}{n!(n+1)!}\gamma(n+1,\nu_c) \tag{27}$$

$$\tilde{\mu}_1 = \frac{L}{v_1}\tilde{\mu}_0 + t_0 e^{-\phi} \sum_{n=0}^{\infty} \frac{\phi^n}{n!(n+1)!}\gamma(n+2,\nu_c) \tag{28}$$

Equations (16), (27), and the quantity, $\{[\tilde{\mu}_1 - (L/v_1)\tilde{\mu}_0]/t_0\}$, in Eq. (28) are shown as a function of τ in Figs. 5 through 7. As $\phi \to 0$, $\tilde{\mu}_0$ approaches a step change at $\tau = 0$ and both $t_0 c_{i1}(L,\tau)$ and $\{[\tilde{\mu}_1 - (L/v_1)\tilde{\mu}_0]/t_0\}$ approach zero. As $\phi \to \infty$, $t_0 c_{i1}(L,\tau)$ approaches a unit impulse at $\tau = 1$ and both $\tilde{\mu}_0$ and $\{[\tilde{\mu}_1 - (L/v_1)\tilde{\mu}_0]/t_0\}$ approach a step change at $\tau = 1$. For large values of ϕ, the value of the first normal statistical moment and the retention time (location of peak maximum) become identical. For small values of ϕ and a finite cutoff time, t_c, the relationship among the retention time and the moments must be evaluated carefully. Other consequences of these results are presented in detail elsewhere (*2*).

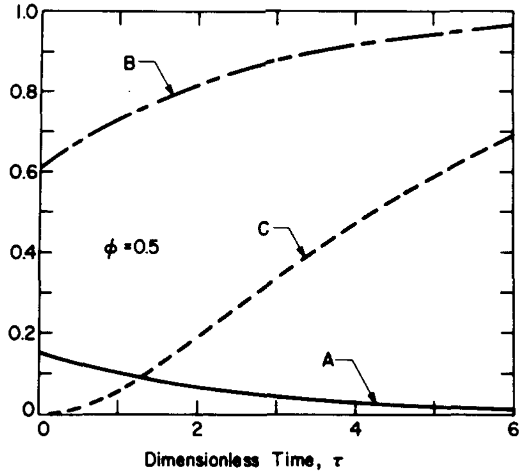

FIG. 5. Plot of Eq. (16) [Curve A], Eq. (27) [Curve B], and the quantity $[\tilde{\mu}_1 - (L/v_1)\tilde{\mu}_0]t_0$ [Curve C] as a function of τ for $\phi = 0.5$.

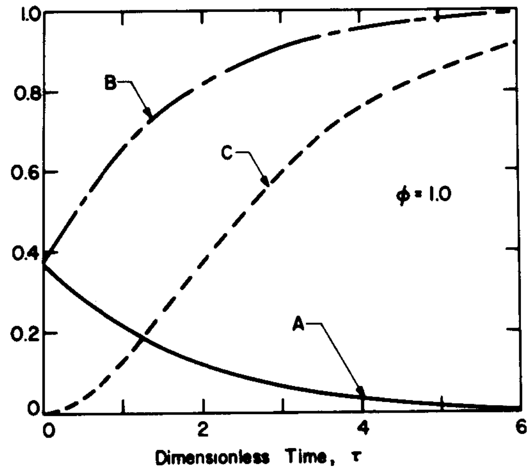

FIG. 6. Plot of Eq. (16) [Curve A], Eq. (27) [Curve B], and the quantity $[\bar{\mu}_1 - (L/v_1)\bar{\mu}_0]/t_0$ [Curve C] as a function of τ for $\phi = 1.0$.

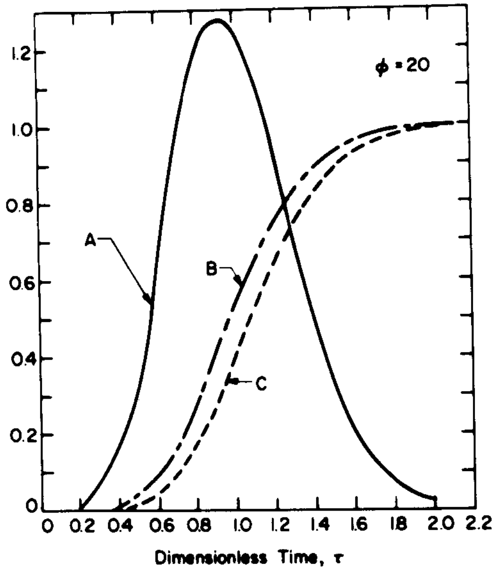

FIG. 7. Plot of Eq. (16) [Curve A], Eq. (27) [Curve B], and the quantity $[\bar{\mu}_1 - (L/v_1)\bar{\mu}_0]/t_0$ [Curve C] as a function of τ for $\phi = 20$.

NORMAL MOMENTS

The normal moments, μ_m', can be calculated from the partial normal moments, $\tilde{\mu}_m$, by taking the following limit,

$$\mu_m' = \lim_{t_c \to \infty} \tilde{\mu}_m \tag{29}$$

By the application of the following relationships,

$$\lim_{\nu_c \to \infty} \gamma(n + 1, \nu_c) = n! \tag{30}$$

$$\lim_{\nu_c \to \infty} \gamma(n + 2, \nu_c) = (n + 1)! \tag{31}$$

$$\sum_{n=0}^{\infty} \frac{\phi^n}{n!} = e^\phi \tag{32}$$

$$\sum_{n=0}^{\infty} \frac{\phi^{n+1}}{(n + 1)!} = e^\phi - 1 \tag{33}$$

Equations (27) and (28) reduce to

$$\lim_{\tau_c \to \infty} \tilde{\mu}_0 = 1 \tag{34}$$

$$\lim_{\tau_c \to \infty} \tilde{\mu}_1 = \frac{L}{v_1} + t_0 = \frac{L}{v_1}\left(1 + \kappa_{i2}\frac{\epsilon_2}{\epsilon_1}\right) \tag{35}$$

We have thus shown that correct results are obtained for the zeroth and first normal moments when $\tau_c \to \infty$. We further observe that the integral summations in Eqs. (27) and (28) are the contributions to the zeroth and first moments from the mass transfer process.

RETENTION TIME

The retention time, τ_R, is that value of τ for which the elution curve of Eq. (16) is a maximum (or that value for which the first derivative with respect to τ is zero). This time can be obtained as a function of ϕ by solving the following equation,

$$\frac{I_1(2\phi\sqrt{\tau_R})}{I_0(2\phi\sqrt{\tau_R})} = \frac{\phi\sqrt{\tau_R}}{1 + \phi\tau_R} \tag{36}$$

Use of the small-value approximation to the Bessel functions, in which the first two terms of the approximation are included, simplifies Eq. (36) to

$$\tau_R \approx \frac{1}{\phi}\left(1 - \frac{2}{\phi}\right) \qquad \text{(small } \phi\text{)} \qquad (37)$$

Equation (37) clearly indicates that no peak in the elution curve will develop for values of ϕ less than 2. The development of the peak as ϕ is increased beyond 2 is shown in Fig. 8.

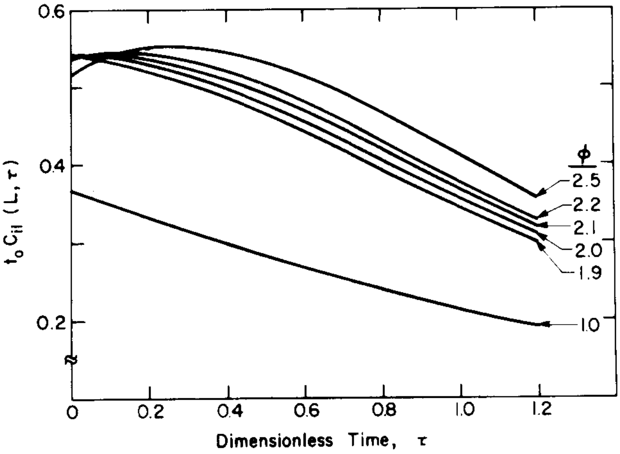

FIG. 8. Plot of Eq. (16) as a function of τ for values of ϕ near 2.0.

In Fig. 9, the dimensionless retention time, τ_R, is plotted versus the inverse of ϕ. As indicated by Eqs. (9) through (11), τ_R may be interpreted as a dimensionless retention (or elution) volume and ϕ^{-1} as a dimensionless flow rate. This can most clearly be seen if we recast Eqs. (9) and (11) into the following forms,

$$\tau_R = \frac{\pi R^2 v_1 t_R - \pi R^2 L}{2\pi a R L \kappa_{i2}} = \frac{V_R - V_C}{2\pi a R L \kappa_{i2}}$$

$$\phi^{-1} = \frac{\pi R^2 v_1}{\frac{8}{3}\frac{D_{i2}}{a^2} \cdot 2\pi a R L \kappa_{i2}} = \frac{Q}{\frac{8}{3}\frac{D_{i2}}{a^2} \cdot 2\pi a R L \kappa_{i2}}$$

where V_R is the retention volume, V_C is the column void volume, and Q is the volumetric gas flow rate (units of cm^3/sec). Thus, as the velocity v_1 increases, ϕ^{-1} increases and τ_R decreases, a conclusion that

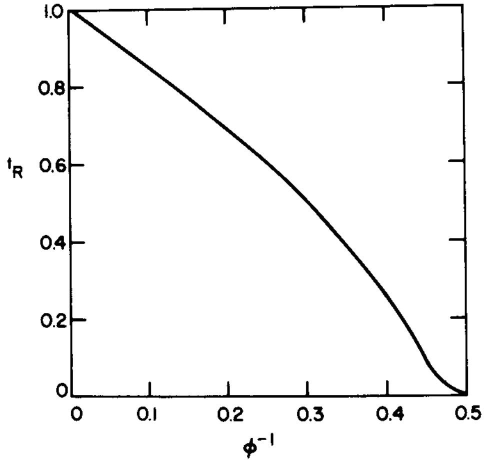

FIG. 9. Solution of Eq. (36).

has experimental support in the data of Oberholtzer and Rogers (*4*) and Little and Pauplis (*3*). Further, a longer column or a lower flow rate decreases ϕ^{-1} and thereby enhances the development of a peak. These effects on peak development have been discussed by Habgood and MacDonald (*6*), who arrived at their conclusions in a different manner.

For large values of ϕ, the dimensionless retention time can be obtained from the large value approximation to Eq. (16)

$$t_0 c_{i1}(L,\tau) \approx \sqrt{\frac{\phi}{4\pi}} \frac{\exp\left[-\phi(1-\sqrt{\tau})^2\right]}{\tau^{3/4}} \qquad \text{(large } \phi) \qquad (38)$$

The impulse at $\tau = 0$ has been neglected since its magnitude is negligible for large ϕ. Equation (38) is shown as the dashed line in Fig. 3; the approximation to Eq. (16) is quite good for large values of ϕ. The value of the peak height is given by the equation,

$$t_0 c_{i1}(L,1) = \sqrt{\frac{\phi}{4\pi}} \qquad \text{(large } \phi) \qquad (39)$$

The value of τ_R from Eq. (38) is

$$\tau_R = 1 - \tfrac{3}{2}\phi^{-1} \qquad \text{(large } \phi) \qquad (40)$$

which, in terms of V_R, V_C, and Q, can be recast as

$$V_R = V_C\left(1 + \frac{2a}{R}\kappa_{i2}\right) - \frac{9}{16}\frac{a^2}{D_{i2}}Q \qquad \text{(large } \phi) \qquad (41)$$

Equation (41) describes the results given in Figs. (3) and (4) in the paper by Oberholtzer and Rogers (*4*) and indicates that a straight line with a negative slope is to be expected.

By making suitable approximations and using Eq. (38), it can be shown that

$$\text{NTP} = \frac{\phi}{2}\left(1 + \frac{L/v_1}{t_0}\right)^2 = \frac{\phi}{2}\left(1 + \frac{1}{\dfrac{2a}{R}\kappa_{i2}}\right)^2 \qquad \text{(large } \phi) \qquad (42)$$

and

$$\text{HETP} = \frac{2L}{\phi}\,\frac{1}{\left(1 + \dfrac{L/v_1}{t_0}\right)^2} = \tfrac{3}{4}v_1\frac{a^2}{D_{i2}}\,\frac{\dfrac{2a}{R}\kappa_{i2}}{\left(1 + \dfrac{2a}{R}\kappa_{i2}\right)^2} \qquad \text{(large } \phi) \qquad (43)$$

where NTP and HETP are the number of theoretical plates and height equivalent of a theoretical plate, respectively. The similarity between these equations and previous ones, such as that of Giddings (*12*), is noted. Details of the derivations are available upon request to the authors.

MOBILE PHASE RESISTANCE TO MASS TRANSFER

The effect of resistance to mass transfer in the mobile phase may also be incorporated into the above solutions by noting that

$$\hat{G} \equiv \frac{\hat{c}_{i2|Av}}{\hat{c}_{i1}} = \frac{\hat{c}_{i2|Av}}{\hat{c}^*_{i1}} \cdot \frac{\hat{c}^*_{i1}}{\hat{c}_{i1}} \qquad (44)$$

If k_f is the mass transfer coefficient (units of cm/sec), the flux-matching condition at the stationary-mobile phase interface is

$$k_f(c_{i1} - c^*_{i1}) = D_{i2}\left.\frac{\partial c_{i2}}{\partial y}\right|_{y=a} \qquad (45)$$

where $c_{i1} - c^*_{i1}$ is the concentration drop across a very thin film near the surface of the stationary phase. The resulting expressions for $\hat{G}$ are

$$\hat{G} = \kappa_{i2}\frac{\tanh qa}{qa} \cdot \frac{1}{1 + \dfrac{\kappa_{i2}}{Nu}\, qa \tanh qa} \qquad \text{Distributed} \qquad (46)$$

$$\hat{G} = \kappa_{i2} \frac{\dfrac{8}{3}\dfrac{D_{i2}}{a^2}\dfrac{1}{1+\dfrac{8}{3}\dfrac{\kappa_{i2}}{Nu}}}{p+\dfrac{8}{3}\dfrac{D_{i2}}{a^2}\dfrac{1}{1+\dfrac{8}{3}\dfrac{\kappa_{i2}}{Nu}}} \qquad \text{Discrete approximation} \qquad (47)$$

where $Nu = k_f a/D_{i2}$ is a Nusselt number for mass transfer.

Equation (46) indicates that a substantially different function of p must be inverted to obtain the elution curve when a distributed representation of the liquid film is employed. On the other hand, Eq. (47) states that the parameter ϕ must simply be corrected by the factor $1/[1 + (8/3)(\kappa_{i2}/Nu)]$ when the discrete description is used. As $k_f \rightarrow \infty$, this factor approaches unity and as $k_f \rightarrow 0$, it approaches zero. The curves shown in Figs. 3 and 4 in Ref. *2* therefore incorporate the effect of mobile-phase resistance to mass transfer, provided that this effect is included in the calculation of ϕ.

CONCLUSIONS

We have shown that the elution curve shape and its moments are characterized, at least for linear chromatography, by a single dimensionless group, ϕ, which is a measure of the rate of mass transfer into the stationary phase by diffusion relative to the rate of mass transfer in the axial direction by convection. Both a distributed and a lumped description of the liquid film are presented; a numerical inversion of the distributed description is shown. The lumped, or discrete, description for the liquid film is, in a sense, a one-term approximation to the distributed representation; closed form solutions are given for the elution curve and the zeroth and first partial normal moments. The dimensionless retention time, τ_R, is shown as a function of ϕ and the results compared to the recently published experimental observations of other investigators. The effect of a stationary-phase resistance to mass transfer is also considered.

The relationship among the retention time, elution curve, and the zeroth and first partial normal moments can be evaluated quantitatively by means of the equations presented in this paper, even under conditions in which severe lateral mass transfer control exists. Furthermore, the results show that the first normal moment is *not* invariant with respect to lateral kinetic phenomena when proper account is taken of the experimental restriction of a finite cutoff time.

List of Symbols

a	thickness of liquid film (cm)
$A_\perp$	lateral cross-sectional area (cm^2)
c	concentration (moles/cm^3)
$\hat{c}$	Laplace transform of concentration
$\hat{c}\vert_{Av}$	Laplace transform of average concentration
c^*	interfacial concentration (moles/cm^3)
$\hat{c}^*$	Laplace transform of interfacial concentration
D	diffusion coefficient (cm^2/sec)
$\hat{G}$	column characteristic
k_f	mass-transfer coefficient (cm/sec)
K	distribution coefficient (moles/moles)
L	column length (cm)
n	series variable
Nu	Nusselt number
p	Laplace transform variable
q	defined by Eq. (7)
Q	volumetric flow rate (cm^3/sec)
R	column radius to surface of stationary phase (cm)
t	time (sec)
t_0	defined by Eq. (10) (sec)
v	defined by Eq. (25)
v_1	velocity of mobile phase (cm/sec)
V_C	column void volume (cm^3)
V_R	retention volume (cm^3)
z	axial Cartesian coordinate (cm)

Greek Letters

γ	gamma function
ϵ	volume fraction (cm^3/cm^3)
κ	partition coefficient (moles/cm^3:moles/cm^3)
μ'_m	mth normal statistical moment (sec^m)
$\tilde{\mu}_m$	mth partial normal statistical moment (sec^m)
τ	defined by Eq. (9)
ϕ	defined by Eq. (11)

Subscripts

c	cutpoint

i	component i
is	component i in environment s (i.e., partition state $\boxed{i:s}$)
m	power in computation of moments
R	retention value
s	environment s
$i1, i2, i3$	specific partition states
1, 2	specific phases

REFERENCES

1. J. E. Funk and P. R. Rony, *Separ. Sci.*, **6**, 365 (1971).
2. P. R. Rony and J. E. Funk, *Proceedings of the Sixth International Symposium on Advances in Chromatography,* Department of Chemistry, Univ. of Houston, Houston, Texas, 1970, p. 59.
3. J. N. Little and W. J. Pauplis, *Separ. Sci.*, **4**, 513 (1969).
4. J. E. Oberholtzer and L. B. Rogers, *Anal. Chem.*, **41**, 1590 (1969).
5. R. N. Kelley and F. W. Billmeyer, Jr., *Ibid.*, **42**, 399 (1970).
6. H. W. Habgood and W. R. MacDonald, *Ibid.*, **42**, 543 (1970).
7. P. Schneider and J. M. Smith, *A. I. Ch. E. Journal,* **14**, 762 (1968).
8. O. Wing, *Computing,* **2**, 153 (1967).
9. J. E. Funk and G. Houghton, *J. Chromatogr.*, **6**, 193 (1961).
10. A. Erdelyi, *Tables of Integral Transforms*, Vol. 1, McGraw-Hill, New York, 1954, p. 244.
11. H. B. Dwight, *Tables of Integrals and Other Mathematical Data,* Macmillan, New York, 1961.
12. J. C. Giddings, *J. Phys. Chem.*, **68**, 184 (1964).

Received by editor August 27, 1970